

Effect of Laser Beam Overlap Rate on Mechanical Properties of Aluminum Alloy Arc Welding with Laser Peening

Jae-Ook Jeon ¹, Ye-Sol Yun ¹, Moo-Keun Song ², Pyeong-Soo Kim ³ and Jong-Do Kim ^{1,*}

¹ Division of Marine System Engineering, Korea Maritime & Ocean University, Busan 49112, Republic of Korea; the_brilliant@nate.com (J.-O.J.); yesol4037@naver.com (Y.-S.Y.)

² Korea Research Institute of Decommissioning, Gyeongju City 38120, Republic of Korea; mksong@krid.re.kr

³ Hanjo Co., Ltd., Busan 606033, Republic of Korea; pskim2000@naver.com

* Correspondence: jdkim@kmou.ac.kr

Abstract: This study aims to investigate the effect of the laser beam overlap rate on the mechanical properties of Al3003 aluminum alloy arc weldment with laser peening. To determine the optimal laser beam overlap rate for laser peening of the weldment, peening experiments were conducted on bead-welded and butt-welded specimens with varying overlap rates, and the effect of the beam overlap rate was analyzed. As the overlap rate increased, the residual stress changed from tensile to compressive, with the highest level of compressive residual stress at the overlap rate of 75%. Laser peening was performed on the aluminum weldment of the prototype, applying the optimal peening conditions identified earlier. As a result of comparing the residual stress, hardness, and tensile strength of the weld before and after laser peening, it was found that the tensile residual stress in the weldment was improved to a compressive residual stress of about -50 MPa or more. The hardness and tensile strength of the weld increased after peening, and the mechanical properties were also improved.

Keywords: laser peening; aluminum alloy; arc welding; laser beam overlap rate; residual stress



Citation: Jeon, J.-O.; Yun, Y.-S.; Song, M.-K.; Kim, P.-S.; Kim, J.-D. Effect of Laser Beam Overlap Rate on Mechanical Properties of Aluminum Alloy Arc Welding with Laser Peening. *Metals* **2024**, *14*, 1021. <https://doi.org/10.3390/met14091021>

Academic Editor: Vincenzo Crupi

Received: 30 June 2024

Revised: 9 August 2024

Accepted: 4 September 2024

Published: 6 September 2024



Copyright: © 2024 by the authors. Licensee MDPI, Basel, Switzerland. This article is an open access article distributed under the terms and conditions of the Creative Commons Attribution (CC BY) license (<https://creativecommons.org/licenses/by/4.0/>).

1. Introduction

Aluminum alloys are recyclable, eco-friendly materials with excellent thermal conductivity, low temperature properties, and corrosion resistance and are gaining attention in various industries [1]. They are metal materials that can significantly contribute to improving fuel efficiency and reducing pollution by replacing heavy steel materials with lightweight component materials in the transportation field, such as aircraft, automobiles, railway vehicles, and ship containers [2–5]. Recently, lightweight aluminum alloys have also been used in intercoolers for engines used in military vehicles such as tanks, armored vehicles, and self-propelled artillery to improve maneuverability [6,7].

The weldment between the core and housing, the main joint in heat exchangers used in most military vehicles today, is welded by an arc heat source [8,9]. The arc welding process, with its high heat input, causes expansion and contraction of the molten metal as the base and filler metals melt and solidify [10,11]. This creates an overall tensile residual stress in and around the weldment. Such tensile residual stresses in weldments can cause fatigue cracks and stress corrosion cracking, shortening the life of the product [12].

Lastowska et al. [13] studied the potential application of an innovative post-weld finishing method of the butt weld of stainless steel and aluminum alloys. Sathyajith et al. [14] analyzed the effect of laser peening on the arc weldment of Al6066. Sano et al. [15] conducted a study to improve fatigue performance by applying dry laser peening to laser-welded Al 2024-T3. Kong et al. [16] researched laser peening forming effects on 5083 aluminum alloy. Li et al. [17] analyzed the effect of ultrasonic shot peening on the microstructure and properties of variable polarity plasma arc welding joints of 7A52 aluminum alloy. However, few studies have been reported on laser peening for the arc weldment of aluminum 3003.

The heat exchanger consists of an inner core and an outer housing. The core's cooling fins use Al3003, which is relatively inexpensive and has high strength by adding manganese (Mn) to pure aluminum. Al3003 also has the advantage of good moldability, weldability, and corrosion resistance. Al4043 has been used as filler wire material for MIG welding for housing and core assembly. Since the heat exchanger core and housing are welded by the arc heat source, there are some problems in that the amount of heat input is large. So, the molten metal expands and contracts during the melting and solidification process, and tensile residual stress is formed in the weldment. The tensile residual stress of the weldment shortens the life of the product by causing fatigue cracks and stress corrosion cracks [12]. Laser peening is effective in preventing stress corrosion cracking and improving fatigue strength because high compression residual stress is formed by the shock wave of plasma generated by irradiating a short pulse laser with high peak power to the material surface. Therefore, in order to solve the above problems, this study aims to improve the quality and mechanical performance of aluminum welding by applying laser peening technology to the fabrication process of military vehicle engine heat exchangers.

2. Materials and Methods

2.1. Experimental Materials

The arc-welded specimens used in the laser peening experiments were made of Al3003 as the base metal and Al4043 as the filler metal, which were the same materials used for the core of the heat exchanger. Al3003 is made of pure aluminum with the addition of manganese (Mn), which is relatively inexpensive and has high strength with good formability, weldability, and corrosion resistance. Table 1 shows the chemical composition of the base material.

Table 1. Chemical composition of base metal Al3003 and filler metal Al4043.

Material \ Element	Si	Fe	Cu	Mn	Mg	Ti	Others	Al
Al3003 (Base metal)	0.23	0.58	0.12	1.11	0.002	0.015	0.015	Bal.
Al4043 (Filler wire)	4.8	0.1	0.02	-	-	0.01	<0.15	Bal.

The arc-welded specimens before the peening test were prepared as aluminum alloy MIG-welded specimens using the same process conditions as the actual product manufacturing, and the welding conditions were voltage 20 V, current 145 A, and welding speed 7.1 m/s.

The specimens for bead welding and butt welding with a groove angle of 30° were prepared, as shown in Figure 1. The welded specimens were used in the experiment after removing the overlay with a thickness of about 3 mm through milling for laser peening.

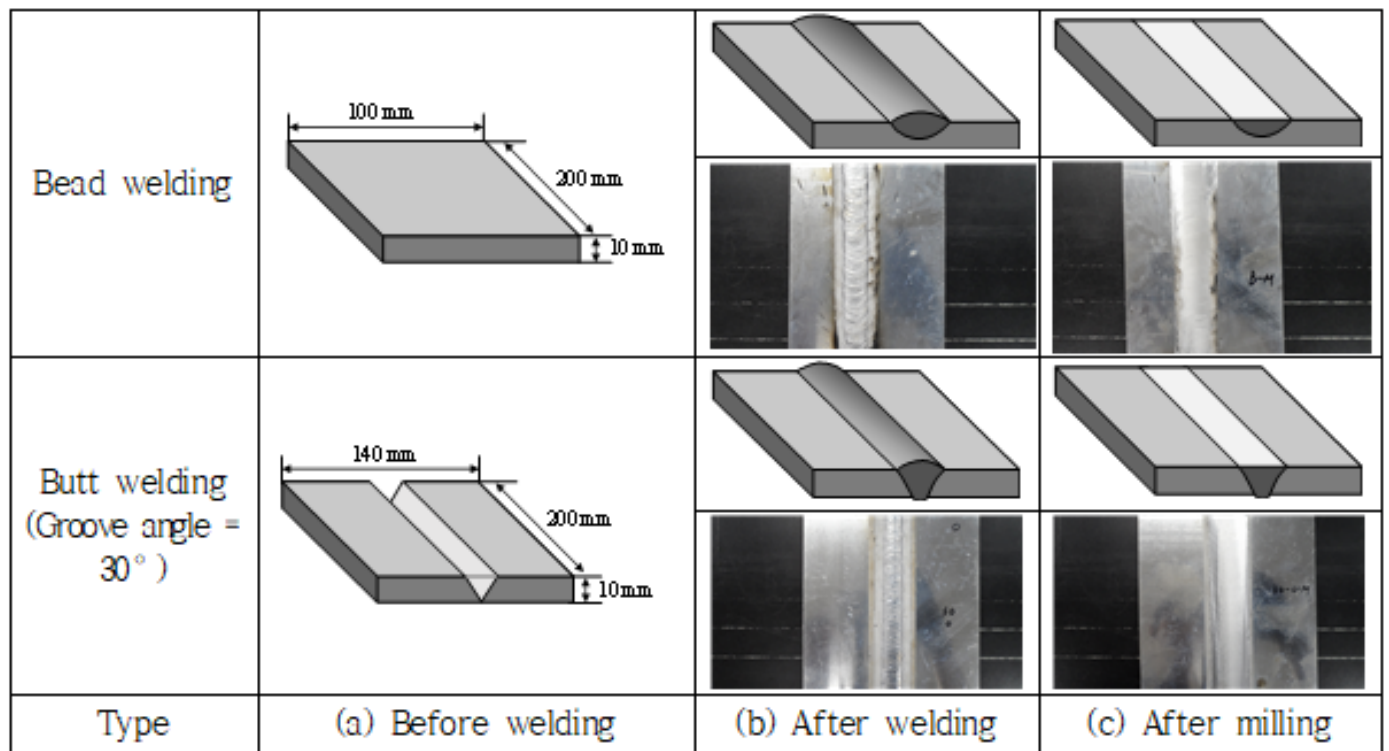


Figure 1. Specimen size and schematic for laser peening.

2.2. Laser Cleaning System and Experimental Approach

The laser used in the laser peening experiment was a Q-switched Nd:YAG laser. The wavelength of the laser could be tuned to 1064 nm and 532 nm, with maximum pulse energies of 1.2 J and 0.5 J, respectively. The laser beam was multimoded with a diameter of 2 mm. Table 2 lists the key specifications of the laser used in the laser peening experiments.

Table 2. Key specifications of the laser used in the laser peening experiment.

Q-Switching Fiber Laser	Value
Output max. energy, E_p	1.2 J (at 1064 nm), 0.5 J (at 532 nm)
Wavelength, λ	1064 nm/523 nm switchable
Pulse duration, τ_p	10 ns
Beam size	2 mm
Laser frequency (f)	10 Hz
Laser beam mode	Multimode

Figure 2 shows the configuration of the laser peening experiment equipment. The experimental equipment consisted of a laser oscillator, laser control panel, laser head, 7-axis arm, and X-Y stage. While the specimen was fixed inside the water tank, the laser beam from the oscillator was irradiated on the surface of the welded specimen located inside the tank. To maximize the effectiveness of laser peening, the surface of the specimen was coated with water to form an inertial tamping layer with a maximum thickness of 2 mm.

Figure 3 shows the schematic of the laser peening area and laser beam overlap. (a) shows the direction of residual stress on the weldment and base metal. (b) shows the laser-peened area on the surface of the welded specimen, with the scan direction perpendicular to the weld direction. In (c), the laser beam and line overlap rate and scan direction are shown. The laser beam irradiated the specimen while overlapping at a constant overlap rate (R). The peening experiments were conducted on specimens while varying the overlap rates to 25%, 50%, and 75%. Water was flowed on the fixed surface of the specimen to form a water layer. The laser wavelength was fixed at 1064 nm, the pulse energy at 1.2 J, and the pulse frequency at 10 Hz.

The bead width was approximately 10 mm, and the laser peening area was 50 mm × 20 mm, including the base material, heat-affected zone, and weldment.

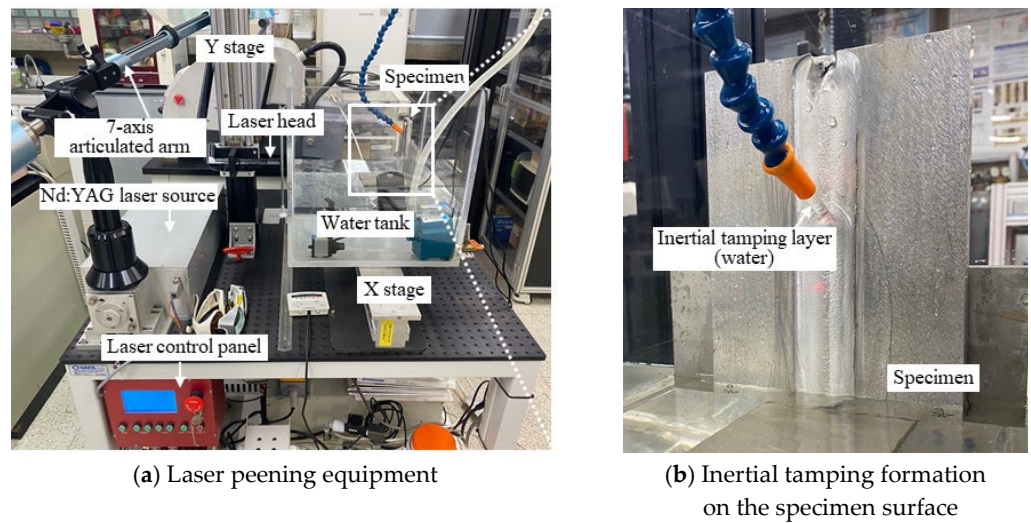


Figure 2. Laser peening equipment configuration.

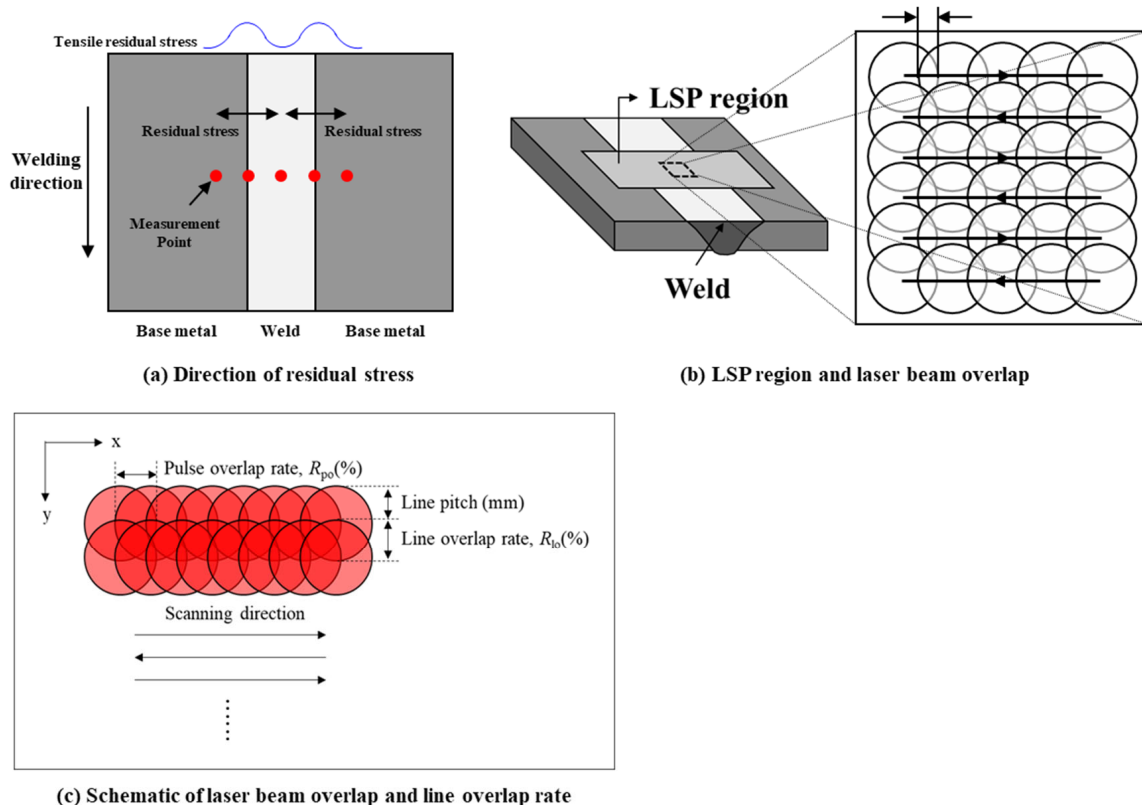


Figure 3. Schematic of the laser peening area and laser beam overlap.

3. Results and Discussion

3.1. Characteristics of Bead Welding and Butt Welding According to Laser Beam Overlap Rate

To obtain the optimal laser beam overlap rate conditions during laser peening of weldments, peening experiments were conducted on bead-welded and butt-welded specimens while varying the overlap rates to 25%, 50%, and 75%.

Figure 4 shows the surface photographs of a bead weldment before and after laser peening as a function of the overlap rate. To analyze the effect of peening, the residual

stresses on the specimen surface before and after peening were measured using an XRD residual stress meter. Three residual stress measurement locations were selected at 5 mm intervals on the left and right sides of the weldment.

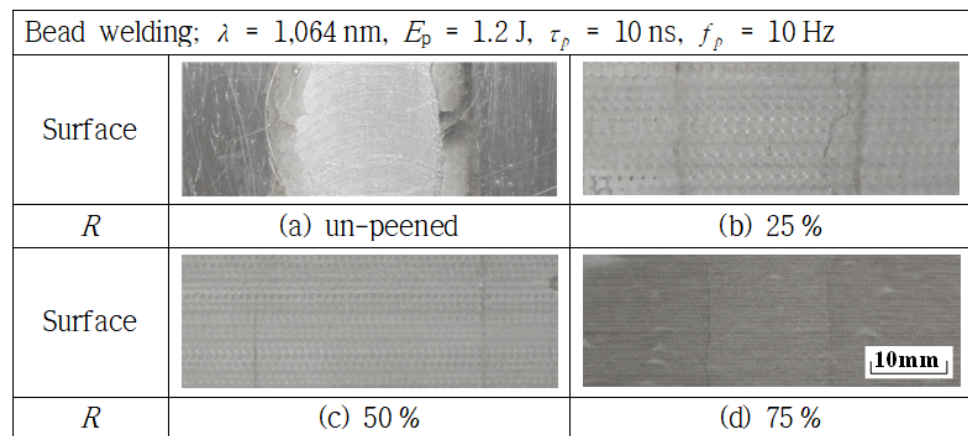


Figure 4. Photograph of the peened surface of a bead-welded specimen as a function of the laser beam overlap rate.

Figure 5 shows the surface residual stress distribution by location on the specimen shown in Figure 4. The pre-peened specimen seemed to have little or no residual stress and a low level of compressive residual stress. At an overlap rate of 25%, the effect of peening was negative, turning the surface residual stress into tensile residual stress. This trend was also observed for an overlap rate of 50%. When the overlap rate was increased to 75%, high levels of compressive residual stress formed at all locations compared to before peening.

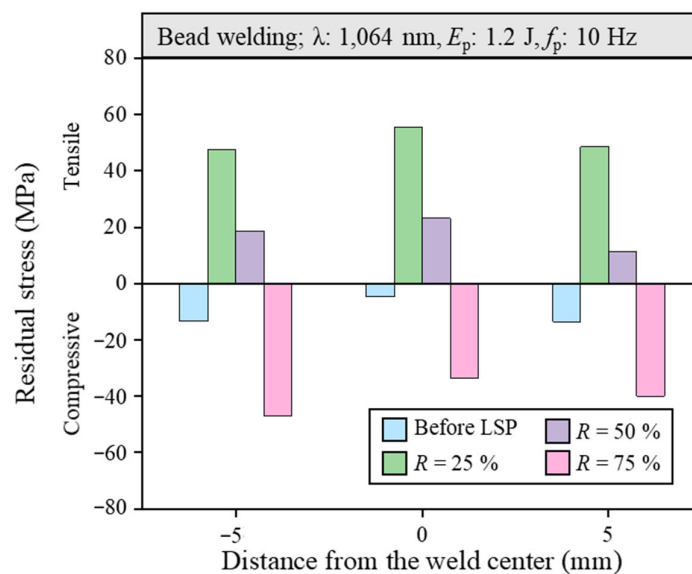


Figure 5. Distribution of residual stresses on the peened surface of a bead-welded specimen as a function of the laser beam overlap rate.

Figure 6 shows the surface photographs of a butt weldment before and after laser peening as a function of the overlap rate, and Figure 7 shows the surface residual stress measurement results by condition. Similar to the results for the bead-welded specimens, tensile residual stresses were formed at 25% and 50% overlap rates, but high levels of compressive residual stress were formed at a 75% overlap rate compared to before laser peening.

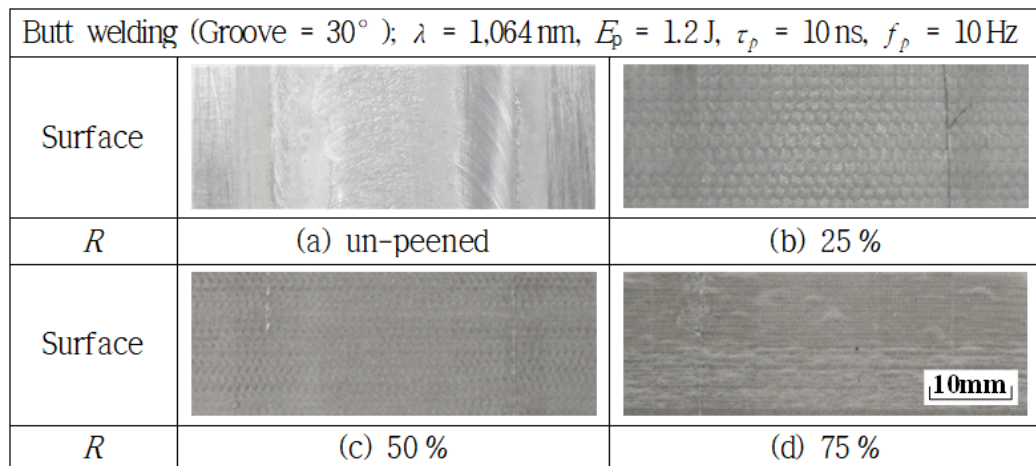


Figure 6. Photograph of the peened surface of a butt-welded specimen as a function of the laser beam overlap rate.

As a result, the highest level of compressive residual stress was formed at a 75% overlap rate. This may have been due to the fact that the impact of the laser shockwave on the surface and inside the material increased as the overlap rate increased.

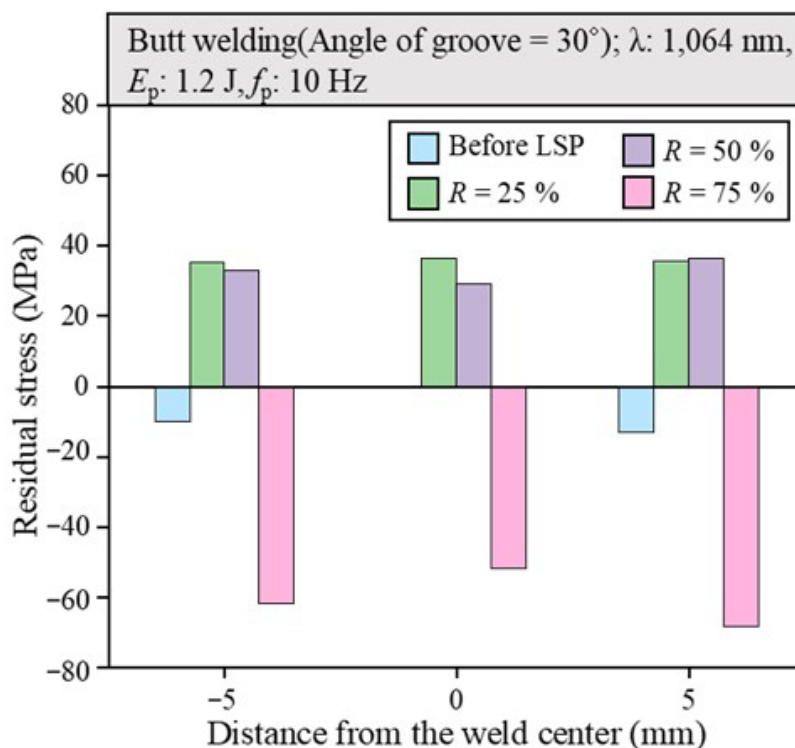
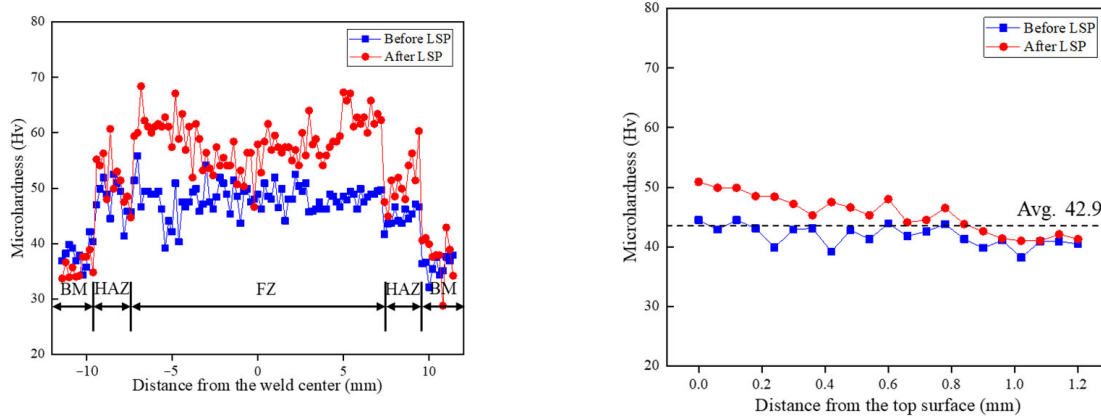


Figure 7. XRD analysis results of the specimen before and after laser cleaning using wave clean beam pattern.

3.2. Changes in Hardness of Aluminum Alloy Welds with Laser Peening Application

To evaluate the mechanical properties of the laser-peened zone, Vickers hardness was measured, and the results are as shown in Figure 8. Figure 8a shows the transverse hardness distribution of the weld measured at a point 60 μm from the surface. The hardness was relatively higher in the molten zone compared to the base metal and the heat-affected zone, which may have been due to the higher hardness of the filler metal (Al4043) than the base metal (Al3003). The hardness of the molten zone increased slightly after laser peening, which

is believed to be due to the densification of the metal structure on the sample surface due to the effect of laser peening. Figure 8b shows the hardness distribution from surface to depth in the molten zone. In the laser-peened specimens, the surface layer had the highest hardness value, and the hardness value decreased with increasing distance from the surface. It also tended to stay close to the average hardness of the base material, 42.9 Hv. This may have been due to the shockwave induced by laser peening being dissipated and weakened by the material as it traveled through the specimen. The hardening depth was about 600 μm .



(a) Microhardness profiles across the weldment (b) Microhardness profiles through depth direction

Figure 8. Comparison of the hardness distribution in the weldment before and after laser peening.

3.3. Effect of Laser Peening on Tensile Strength of Aluminum Alloy Welds

This study was conducted as basic research to improve the performance of aluminum welds by applying eco-friendly laser surface treatment technology to the manufacturing process of military heat exchangers. Therefore, laser cleaning was applied as a pre-welding process, and laser peening was applied as a post-welding process. To analyze the mechanical properties of the welds following the application of laser surface treatment, specimens with no surface treatment, cleaning only, and both cleaning and peening were produced. The specimens were used for tensile testing in accordance with the requirements of ASME BPVC SEC.IX-2019. Three tensile test specimens were tested for each condition, and the average value was calculated to reduce the variance in the experimental results and verify their accuracy.

Figure 9 shows the fracture specimen image and tensile test result graph for the tensile test specimen by condition. In the tensile test, a tensile strength of 77.9 N/mm^2 was measured for the specimen without laser surface treatment (a) and 85.6 N/mm^2 for the specimen with laser cleaning before welding (b). In the specimen with both cleaning and peening applied (c), a tensile strength of 92.6 N/mm^2 was measured, indicating that the application of laser peening increased the tensile strength of the weld. As can be seen in Figure 8, the hardness of the weld was increased due to the effect of laser peening. This increase in surface hardness leads to an increase in shear tensile strength [18]. This can be seen as a result of the reduction in pores in the weldment by laser cleaning before welding and the improvement in residual stress by laser peening after welding.

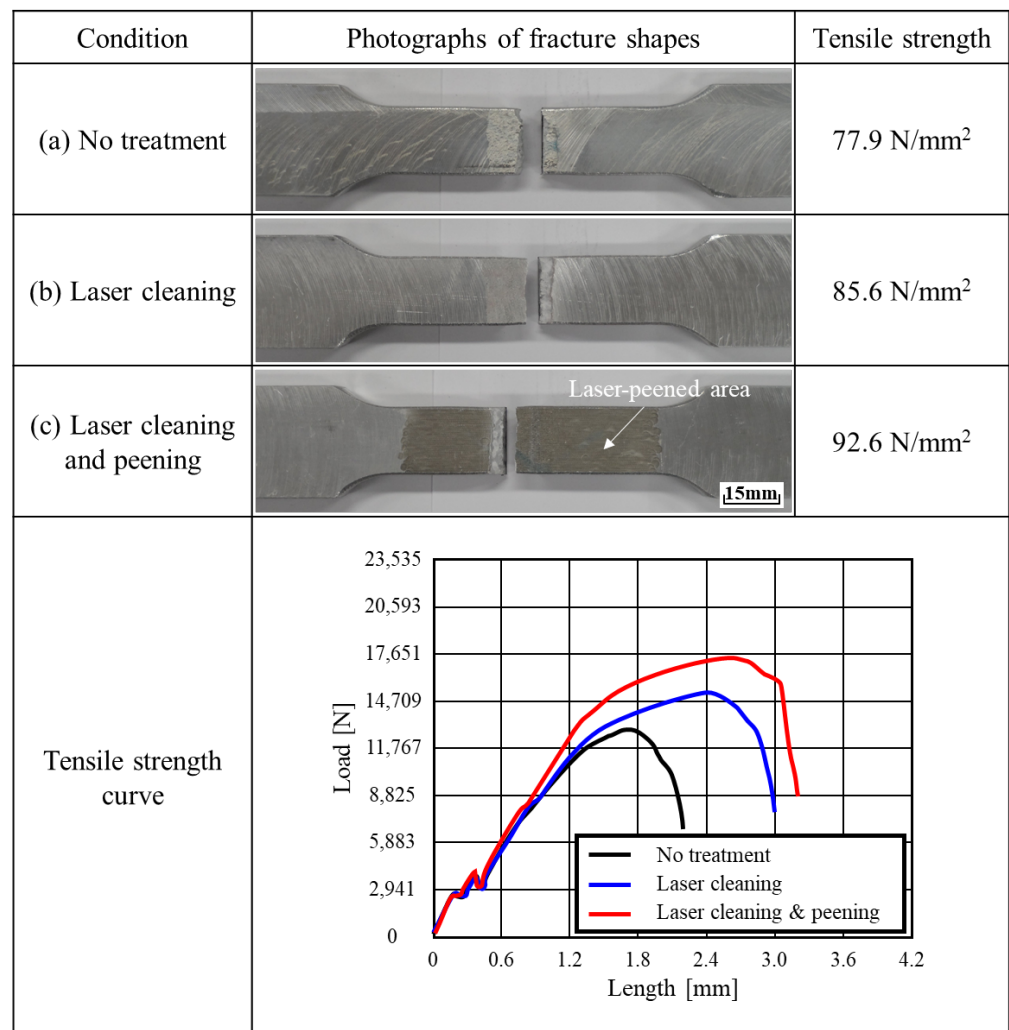


Figure 9. Comparison of tensile test results after laser surface treatment.

Figure 10 shows a cross-section of a tensile test fracture taken by digital microscopy and SEM. The ductile fracture characteristics of the dimpled structure, a stable fracture with a relatively slow propagation speed, were observed in all specimens under all conditions. In the specimen with the lowest tensile strength (a), a large number of pores were observed, which were formed by residual hydrogen gas inside the weldment due to contaminants and an oxidation layer remaining on the surface during welding. These defects were significantly reduced in specimens (b) and (c), which underwent laser peening, due to the elimination of pore formation factors. As a result, the tensile strength was improved by about 7.7 N/mm² in specimen (b) and by 14.7 N/mm² in specimen (c) compared to specimen (a). It was observed that the ductility was improved and the elongation was also increased due to the reduction in defects such as pores in the weld due to the pre- and post-welding processes. This confirmed that laser peening could improve mechanical properties by improving residual stress and increasing tensile strength in the weldment.

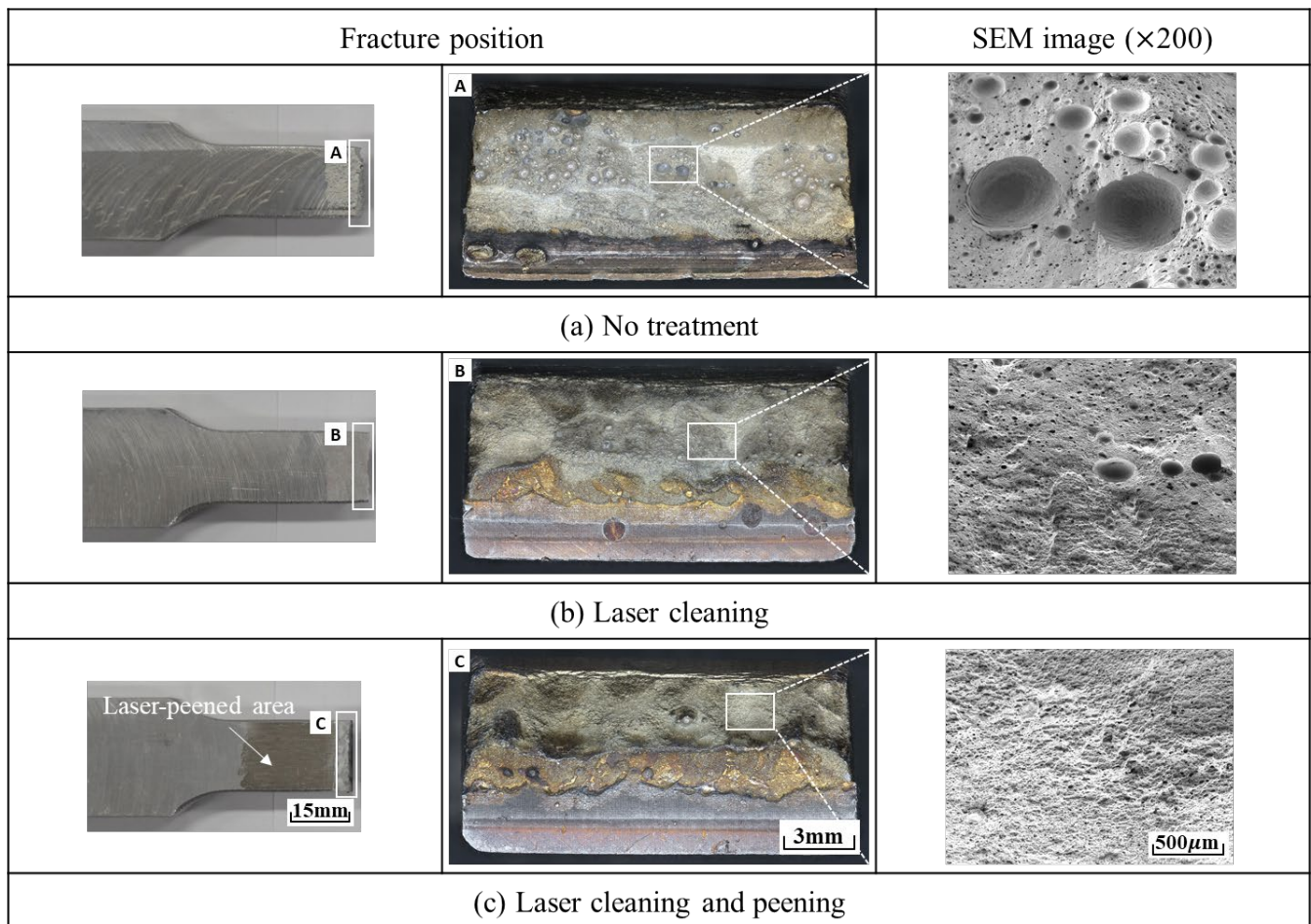


Figure 10. Fracture surface analysis of tensile test specimens by laser surface treatment.

4. Conclusions

A study on the effect of process variables on the improvement of residual stress in the application of laser peening technology to obtain reliable aluminum alloy welds in the manufacture of military heat exchangers led to the following conclusions:

- (1) Aluminum alloy arc welds showed that tensile residual stresses were formed at 25% and 50% overlap rates for both bead-welded and butt-welded zones, but high levels of compressive residual stresses were formed at a 75% overlap rate compared to before laser peening. This may have been due to the fact that the impact of the laser shockwave on the surface and inside the material increased as the overlap rate increased.
- (2) The hardness was relatively higher in the molten zone compared to the base metal and the heat-affected zone, which may have been due to the hardness of the filler metal being higher than that of the base metal. The hardness in the molten zone was found to increase slightly after laser peening. In particular, the surface layer had the highest hardness after laser peening, and the hardness decreased with increasing distance from the surface in the depth direction. The hardening depth was about 600 μm .
- (3) The tensile strength was 77.9 N/mm^2 in the weld without cleaning, 85.6 N/mm^2 in the weld with cleaning only, and 92.6 N/mm^2 in the weld with both cleaning and peening. This suggested that laser peening could improve the mechanical properties of aluminum alloy welds by improving residual stress and tensile strength.

Through this study, the residual stress was improved by applying laser peening to the Al3003 arc weldment of the vehicle heat exchanger. In addition, it was confirmed that the surface hardness and tensile strength of the weldment were improved. The authors are

conducting research on the application of laser cleaning and peening as surface modification technology for weldment in vehicles, ships, and nuclear power plant fields, and it is thought that laser peening can be applied as a surface treatment technology to the post-welding process in various fields.

Author Contributions: Conceptualization, P.-S.K. and J.-D.K.; Validation, M.-K.S. and J.-D.K.; Formal analysis, J.-O.J. and Y.-S.Y.; Investigation, J.-O.J. and Y.-S.Y.; Resources, P.-S.K.; Data curation, J.-O.J. and Y.-S.Y.; Writing—original draft, J.-O.J.; Writing—review and editing, M.-K.S.; Visualization, J.-O.J. and Y.-S.Y.; Supervision, J.-D.K.; Project administration, J.-D.K. All authors have read and agreed to the published version of the manuscript.

Funding: The following are the results of a study on the “Leaders in INdustry-university Cooperation 3.0” Project, funded by the Ministry of Education and the National Research Foundation of Korea. This research was supported by the Industrial Innovation Infrastructure Establishment Project of the Ministry of Trade, Industry and Energy, “Advancement of Manufacturing Equipment Base for E-mobility using Laser Technology” (Project Number 00430048).

Data Availability Statement: The data presented in this study are available on request from the corresponding author. The data are not publicly available due to privacy.

Conflicts of Interest: Author Pyeong-Soo Kim was employed by the company Hanjo Co., Ltd. The remaining authors declare that the research was conducted in the absence of any commercial or financial relationships that could be construed as a potential conflict of interest.

References

1. Raabe, D.; Ponge, D.; Uggowitzer, P.J.; Roscher, M.; Paolantonio, M.; Liu, C.; Antrekowitsch, H.; Kozeschnik, E.; Seidmann, D.; Gault, B.; et al. Making sustainable aluminum by recycling scrap: The science of “dirty” alloys. *Prog. Mater. Sci.* **2022**, *128*, 100947. [[CrossRef](#)]
2. Wazeer, A.; Das, A.; Abeykoon, C.; Sinha, A.; Karmakar, A. Composites for electric vehicles and automotive sector: A review. *Green Energy Intell. Transp.* **2023**, *2*, 100043. [[CrossRef](#)]
3. Santos, J.; Gouveia, R.M.; Silva, F.J.G. Designing a new sustainable approach to the change for lightweight materials in structural components used in truck industry. *J. Clean. Prod.* **2017**, *164*, 115–123. [[CrossRef](#)]
4. Zhu, L.; Li, N.; Childs, P.R.N. Childs, Light-weighting in aerospace component and system design. *Propuls. Power Res.* **2018**, *7*, 103–119. [[CrossRef](#)]
5. Crupi, V.; Epasto, G. Guglielmino, Comparison of aluminium sandwiches for lightweight ship structures: Honeycomb vs. foam. *Mar. Struct.* **2013**, *30*, 74–96. [[CrossRef](#)]
6. Pratomo, A.N.; Santosa, S.P.; Gunawan, L.; Widagdo, D.; Putra, I.S. Design optimization and structural integrity simulation of aluminum foam sandwich construction for armored vehicle protection. *Compos. Struct.* **2021**, *276*, 114461. [[CrossRef](#)]
7. Siengchin, S. A review on lightweight materials for defence applications: Present and future developments. *Def. Technol.* **2023**, *24*, 1–17. [[CrossRef](#)]
8. Chen, Z.; Zhang, Y.; Chi, Y.; Gou, J.; Lin, C.; Lin, Y. Research on morphology, porosity, mechanical properties of 7075 aluminum alloy repaired by arc welding and laser shock forging. *Heliyon* **2023**, *9*, e22791. [[CrossRef](#)] [[PubMed](#)]
9. Wang, J.; Ling, X.; Zhang, W.; Lu, X.; Chen, C. Microstructures and mechanical properties of friction stir welded butt joints of 3003-H112 aluminum alloy to 304 stainless steel used in plate-fin heat exchanger. *J. Mater. Res. Technol.* **2022**, *21*, 3086–3097. [[CrossRef](#)]
10. Chen, C.; Sun, G.; Du, W.; Li, Y.; Fan, C.; Zhang, H. Influence of heat input on the appearance, microstructure and microhardness of pulsed gas metal arc welded Al alloy weldment. *J. Mater. Res. Technol.* **2022**, *21*, 121–130. [[CrossRef](#)]
11. AlShaer, A.W.; Li, L.; Mistry, A. The effects of short pulse laser surface cleaning on porosity formation and reduction in laser welding of aluminium alloy for automotive component manufacture. *Opt. Laser Technol.* **2014**, *64*, 162–171. [[CrossRef](#)]
12. Xu, S.; Chen, J.; Shen, W.; Hou, R.; Wu, Y. Fatigue strength evaluation of 5059 aluminum alloy welded joints Considering welding deformation and residual stress. *Int. J. Fatigue* **2022**, *162*, 106988. [[CrossRef](#)]
13. Łastowska, O.; Starosta, R.; Jabłońska, M.; Kubit, A. Exploring the Potential Application of an Innovative Post-Weld Finishing Method in Butt-Welded Joints of Stainless Steels and Aluminum Alloys. *Materials* **2024**, *17*, 1780. [[CrossRef](#)] [[PubMed](#)]
14. Sathyajith, S.; Kalainathan, S. Effect of laser shot peening on precipitation hardened aluminum alloy 6061-T6 using low energy laser. *Opt. Lasers Eng.* **2012**, *50*, 345–348, ISSN 0143-8166. [[CrossRef](#)]
15. Sano, T.; Eimura, T.; Hirose, A.; Kawahito, Y.; Katayama, S.; Arakawa, K.; Masaki, K.; Shiro, A.; Shobu, T.; Sano, Y. Improving Fatigue Performance of Laser-Welded 2024-T3 Aluminum Alloy Using Dry Laser Peening. *Metals* **2019**, *9*, 1192. [[CrossRef](#)]
16. Kong, C.; Zhang, X.; Chen, G.; Yuan, X.; Liu, B.; Zhu, R. Comprehensive Analysis of Laser Peening Forming Effects on 5083 Aluminum Alloy. *Micromachines* **2024**, *15*, 949. [[CrossRef](#)] [[PubMed](#)]

17. Li, G.; Xu, W.; Liang, Y.; Wang, J. Effect of Ultrasonic Shot Peening on Microstructure and Properties of Variable Polarity Plasma Arc Welding Joints of 7A52 Aluminium Alloy. *J. Mater. Eng. Perform.* **2024**, 1–11. [[CrossRef](#)]
18. Min-Seok, K.; Sung-Jin, P.; Ji-Yeon, S. Investigation of Joint Quality 980 MPa Grade GA Steel Sheet and 5052 Aluminum Alloy by Electromagnetic Self-Piercing Riveting. *J. Weld. Join.* **2023**, *41*, 161–168.

Disclaimer/Publisher’s Note: The statements, opinions and data contained in all publications are solely those of the individual author(s) and contributor(s) and not of MDPI and/or the editor(s). MDPI and/or the editor(s) disclaim responsibility for any injury to people or property resulting from any ideas, methods, instructions or products referred to in the content.